# Theoretical Cluster Studies on the Catalytic Sulfidation of $MoO_3$

**Xue-Rong Shi,[†,‡,§] Jianguo Wang,[*,‡] and Klaus Hermann[*,†]**

*Theory Department, Fritz-Haber-Institut der MPG, Faradayweg 4-6, D-14195 Berlin, Germany, State Key Laboratory of Coal Conversion, Institute of Coal Chemistry, Chinese Academy of Sciences, Taiyuan, Shanxi 030001, People's Republic of China, and Graduate University of the Chinese Academy of Sciences, Beijing 100039, People's Republic of China*

*Received: December 8, 2009; Revised Manuscript Received: February 15, 2010*

Density-functional theory together with large surface clusters is applied to study elementary processes of the catalytic sulfidation of the $MoO_3$(010) surface. For all sites, surface oxygen is found to bind more strongly with its substrate environment than the corresponding sulfur substitute with binding distances that are shorter for oxygen than for sulfur. Sulfur−oxygen exchange reactions are energetically preferred over sulfur adsorption at $MoO_3$(010). The first and second sulfur substitution takes place preferentially at the terminal oxygen site O(1) where the two steps are energetically similar. Further, sulfur binding is found to be facilitated by the existence of surface oxygen vacancies where sulfur substitution takes place preferentially at the terminal oxygen sites O(1) and O(1)′. On the basis of the theoretical results, different sulfidation schemes are considered. They indicate that sulfidation of the $MoO_3$ surface is facilitated by hydrogen participating in the reaction.

## 1. Introduction

Mo-based catalysts, such as $MoS_2$-type, are known to yield high activity for hydrodesulfurization (HDS) and hydrodenitrogenation (HDN) processes and exhibit also high activity for methanation and for the Fischer−Tropsch synthesis of light hydrocarbons from CO hydrogenation.[1−7] $MoS_2$-based catalysts are initially prepared from highly dispersed molybdenum trioxide, $MoO_3$, on high-surface-area supports to which promoters, such as K, Co, or Ni, may be added and are subsequently converted to the catalytically active phase by sulfidation, typically in a $H_2S/H_2$ atmosphere.[8−11] Thus, the sulfidation process of $MoO_3$ forms an essential part of the catalyst preparation, which makes studies on corresponding mechanisms and elementary reaction steps quite important.

The sulfidation process of $MoO_3$ has been extensively studied by experiment.[12,14−18] Scheffer et al.[13] have considered the sulfidation of $MoO_3$ on different supports and find that crystalline $MoO_3$ of low dispersion is relatively difficult to sulfidize. Results from X-ray photoelectron spectroscopy (XPS)[12,14−18] suggest that the sulfidation of $MoO_3$ to $MoS_2$ proceeds via an oxysulfide, $Mo^{4+}OS_x$, appearing initially at the $MoO_3$ surface where the sulfidic species is believed to facilitate the reduction of $MoO_3$ to a $Mo^{4+}$-containing compound. During the sulfidation process, sulfur is assumed to be present as $S^{2-}$, $S_2^{2-}$, or as $SH^-$ species, which is consistent with studies on the thermal decomposition of $(NH_4)_2MoO_2S_2$.[17,18] These studies indicate that bridging $S_2^{2-}$ ligands are formed during the sulfidation of $MoO_3$. They suggest further that hydrogen, $H_2$, does not participate initially, but the sulfidation starts with an exchange of oxygen by sulfur at terminal Mo═O groups of the $MoO_3$ surface. However, a direct reaction between terminal oxygen and $H_2$ to produce oxygen vacancies cannot be excluded. Further, experiments using in situ techniques have shown that both the sulfidation of $MoO_3$ to yield $MoS_2$ and a subsequent re-exposure to air proceed via oxysulfide phases.[8]

Although there is an abundance of experimental work on the sulfidation of $MoO_3$, theoretical studies on these systems are still missing. Therefore, in the present theoretical study, we use density functional theory (DFT) together with gradient-corrected functionals and large cluster models to examine the geometric, energetic, and electronic behavior of oxygen and sulfur adsorbates as well as hydrogen adsorption at local sections of the $MoO_3$(010) substrate surface. The surface clusters are meant to simulate local sections of corresponding catalysts, and the different adsorption scenarios can be considered as model steps of the sulfidation happening at the catalyst surfaces. This may allow a deeper understanding of detailed mechanisms and an interpretation of the experimental results at an atomic level.

In section 2, we describe computational details of the present work, whereas in section 3, we present results of the calculations on oxygen, sulfur adsorption, and O/S exchange at $MoO_3$(010); on hydrogen adsorption; and on possible scenarios of the $MoO_3$ surface sulfidation. Finally, in section 4, we summarize our results and conclusions.

## 2. Computational Details

Bulk $MoO_3$ forms an orthorhombic crystal lattice with a layer structure of weakly binding oxide bilayers parallel to (010) netplanes; see Figure 1a. Each bilayer consists of two interleaved planes of distorted $MoO_6$ octahedra sharing a corner, while octahedra of adjacent planes share edges.[19,20] The (010) surface of $MoO_3$ is energetically the most stable and represents the preferred cleavage plane of the crystal, exposing three differently coordinated oxygen species; see Figure 1a,b. The terminal molybdenyl oxygen species, O(1), is connected with one molybdenum atom by a bond directed almost perpendicular to the surface plane. Bridging oxygen, O(2), is coordinated asymmetrically to two Mo atoms with bonds along the (100) direction, while O(3) is coordinated symmetrically to two metal centers along the (001) direction in the upper part of the bilayer and, with a longer distance, to one molybdenum in the lower

* To whom correspondence should be addressed. E-mail: hermann@fhi-berlin.mpg.de (K.H.), iccjgw@sxicc.ac.cn (J.W.).
† Fritz-Haber-Institut der MPG.
‡ Institute of Coal Chemistry, Chinese Academy of Sciences.
§ Graduate University of the Chinese Academy of Sciences.

10.1021/jp911639e 
Published on Web 03/24/2010

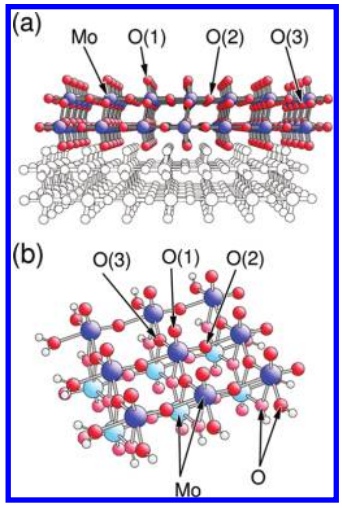


**Figure 1.** (a) Geometric structure of orthorhombic $MoO_3$ bulk with netplane stacking along the (010) direction. The figure includes two physical bilayers. Molybdenum and oxygen atoms are shown by large and small balls, respectively, where those of the topmost bilayer are emphasized by shading. Molybdenum and differently coordinated oxygen centers, O(1), O(2), and O(3), are labeled accordingly. (b) Geometric structure of the $Mo_{15}O_{56}H_{22}$ cluster representing a bilayer section at the perfect $MoO_3(010)$ surface. Oxygen and molybdenum atoms of the lower network within the bilayer are shown with lighter colors. Saturator hydrogen at the cluster periphery is represented by very small balls.

part. In this study, local sections of the $MoO_3(010)$ surface are modeled by corresponding clusters where hydrogen is used to saturate dangling bonds at peripheral oxygen sites.[19,21,22] Here, we consider a $Mo_{15}O_{56}H_{22}$ surface cluster (see Figure 1b) to describe properties of the $MoO_3(010)$ surface, including oxygen vacancies (simulated by $Mo_{15}O_{55}H_{22}$ clusters) and substitutional sulfur adsorbates (modeled by $Mo_{15}O_{55}SH_{22}$) as well as hydrogen adsorption (modeled by $Mo_{15}O_{56}H_{22}H_{(1,2)}$) at the differently coordinated oxygen sites, O(1), O(2), and O(3). In the calculations, the local cluster environments near vacancies and adsorbates are always optimized geometrically to account for surface relaxation in response to local perturbations.

Electronic ground states and derived properties of the clusters are calculated using density functional theory (DFT) together with generalized gradient-corrected exchange and correlation functionals according to Perdew, Burke, and Ernzerhof (RPBE).[23,24] The Kohn−Sham orbitals are represented by linear combinations of atomic orbitals (LCAO) using extended basis sets of contracted Gaussians. For the ground-state calculations and in corresponding geometry optimizations, oxygen, sulfur, and hydrogen are represented by all-electron DZVP basis sets ([3s2p1d] for O, [4s3p1d] for S, and [4s3p] for H), whereas for saturator hydrogen, a smaller basis set ([2s]) is used. Molybdenum is represented by an effective core potential (ECP) together with a valence basis set [6s5p4d] for the 14 outermost valence electrons. All calculations are performed using the DFT cluster code StoBe.[25]

Binding and adsorption energies are evaluated from differences of corresponding cluster total energies. Here, surface binding energies $E_{sb}(O)$ of oxygen, which have to be overcome when surface oxygen is removed from the substrate, forming an oxygen vacancy, are defined by

$$E_{sb}(O) = E_{tot}(Sub) - E_{tot}(Sub_{Ovac}) - E_{tot}(O) \quad (1)$$

with Sub reflecting the cluster of the perfect $MoO_3(010)$ substrate, $Sub_{Ovac}$ denoting the substrate cluster with a surface oxygen vacancy after relaxation, and atomic oxygen considered in its triplet ground state. Thus, $E_{sb}(O)$ can also be considered an oxygen vacancy energy at the substrate surface. Further, surface binding energies $E_{sb}(S)$ of sulfur substituting surface oxygen are given by

$$E_{sb}(S) = E_{tot}(Sub_{Ovac}S) - E_{tot}(Sub_{Ovac}) - E_{tot}(S) \quad (2)$$

with $Sub_{Ovac}S$ denoting the (relaxed) $MoO_3(010)$ substrate cluster with one surface oxygen replaced by sulfur and atomic sulfur considered in its triplet ground state. Obviously, $E_{sb}(O)$ and $E_{sb}(S)$ assume negative values when the O,S species stabilize at their respective equilibrium positions at the substrate surface. The oxygen-by-sulfur substitution energy $E_{S/O}$ at the surface, defined with respect to gas-phase $H_2O$ and $H_2S$, is given by

$$E_{S/O} = E_{tot}(Sub_{Ovac}S) + E_{tot}(H_2O) - [E_{tot}(Sub) + E_{tot}(H_2S)] \quad (3)$$

where negative $E_{S/O}$ values describe exothermic and positive values endothermic substitution. Further, energies $E_{ads}(Ad)$ for sulfur and hydrogen adsorption are defined by

$$E_{ads}(Ad) = E_{tot}(SubAd) - E_{tot}(Sub) - E_{tot}(Ad) \quad (4)$$

where SubAd denotes the $MoO_3(010)$ substrate cluster with adsorbates sulfur or hydrogen added. Here, negative values of $E_{ads}(Ad)$ result in the adsorbates stabilizing at the surface. Sulfur adsorbed above oxygen at a surface site may also be considered as a SO species adsorbed at the corresponding oxygen vacancy site. This suggests the definition of surface binding energies $E_{sb}(SO)$ of the SO species filling formally a surface oxygen vacancy by

$$E_{sb}(SO) = E_{tot}(SubS) - E_{tot}(Sub_{Ovac}) - E_{tot}(SO) \quad (5)$$

where SubS refers to a cluster of the perfect $MoO_3(010)$ substrate with sulfur added, $Sub_{Ovac}$ describes the substrate cluster with a surface oxygen vacancy, and molecular SO is considered in its triplet ground state. Likewise, hydrogen adsorption at the perfect $MoO_3(010)$ substrate, involving one or two hydrogen atoms, may lead to surface OH and $H_2O$ groups whose binding with the substrate at an oxygen vacancy site can be defined by

$$E_{sb}(OH) = E_{tot}(SubH) - E_{tot}(Sub_{Ovac}) - E_{tot}(OH) \quad (6)$$

and

$$E_{sb}(H_2O) = E_{tot}(SubH_2) - E_{tot}(Sub_{Ovac}) - E_{tot}(H_2O) \quad (7)$$

where, in both cases, Sub refers to the perfect substrate. Further, hydrogen adsorption at sulfur sites of the sulfidic $MoO_3(010)$ substrate, involving one or two hydrogen atoms, may lead to

surface SH and $H_2S$ groups whose binding with the substrate at an oxygen vacancy site can be defined by

$$E_{sb}(SH) = E_{tot}(SubH) - E_{tot}(Sub_{Ovac}) - E_{tot}(SH) \quad (8)$$

and

$$E_{sb}(H_2S) = E_{tot}(SubH_2) - E_{tot}(Sub_{Ovac}) - E_{tot}(H_2S) \quad (9)$$

where Sub refers to the sulfidic substrate. Finally, the adsorption of sulfur at the substrate surface can be evaluated by either starting from atomic sulfur in gas phase, where the adsorption energy is defined by eq 4 with Ad = S, or starting from gas-phase $H_2S$ to yield adsorbed sulfur and gas phase $H_2$. The adsorption energy $E_{ads}(S)'$ of the latter process is defined by

$$E_{ads}(S)' = E_{tot}(SubS) + E_{tot}(H_2) - E_{tot}(Sub) - E_{tot}(H_2S) \quad (10)$$

where SubS refers to a cluster of the perfect $MoO_3(010)$ substrate with sulfur added. Definitions 1−10 will be used in the discussion below.

## 3. Results and Discussion

**3.1. Surface Binding of Oxygen and Sulfur at the $MoO_3$(010) Surface.** ***3.1.1. Binding at the Perfect $MoO_3$(010) Surface.*** Table 1 lists calculated surface binding energies $E_{sb}(O)$ of oxygen for different oxygen sites, O(1), O(2), and O(3), at the perfect $MoO_3(010)$ surface where the energies are obtained according to definition 1. Here, the substrate cluster $Mo_{15}O_{56}H_{22}$ is used as the initial surface cluster (see Figure 1b) and corresponding oxygen vacancy clusters $Mo_{15}O_{55}H_{22}$ are applied with Mo and O atoms near the vacancy allowed to relax in response to the missing surface oxygen. Further, atomic oxygen is taken as reference. Obviously, oxygen is bound very strongly at the oxide surface where $E_{sb}(O)$ is largest in absolute magnitude for the 3-fold-coordinated O(3) site, smaller for 2-fold-coordinated O(2), and the smallest for singly coordinated O(1). This agrees qualitatively with results from previous cluster calculations.[19] However, the published $E_{sb}(O)$ values (vacancy energies) are smaller in absolute magnitude by 0.5 eV (O(1) and O(2) sites) and by 0.1 eV (O(3) site) compared with the present results. The difference is explained by the present calculations, allowing a larger number of atoms to relax near the vacancy, which yields a larger energy gain due to relaxation.

**TABLE 1: Surface Binding Energies, $E_{sb}(X)$, X = O, S, at the Perfect $MoO_3$(010) Surface for Different Oxygen Sites Obtained from Cluster Model Calculations; See Text. The Table Includes Equilibrium Distances $d$(X−Mo) of the Two Species with Respect to Their Nearest Mo Neighbors at the Surface[b]**

| site | O(1) | O(2) | O(3) |
|---|---|---|---|
| $E_{sb}(O)$ | −5.36 | −5.64 | −6.45 |
| $d$(O−Mo) | 1.70 | 1.75 | 1.95 |
| $E_{sb}(S)$ | −3.38 | −1.37 | −2.75 |
| $d$(S−Mo) | 2.15 | 2.11 | 2.29 |
| $E_{S/O}$[a] | −0.15 | 2.14 | 1.57 |

[a] $E_{S/O}$ denotes oxygen/sulfur substitution energies; see text. [b] All energies are given in eV, distances in Å.

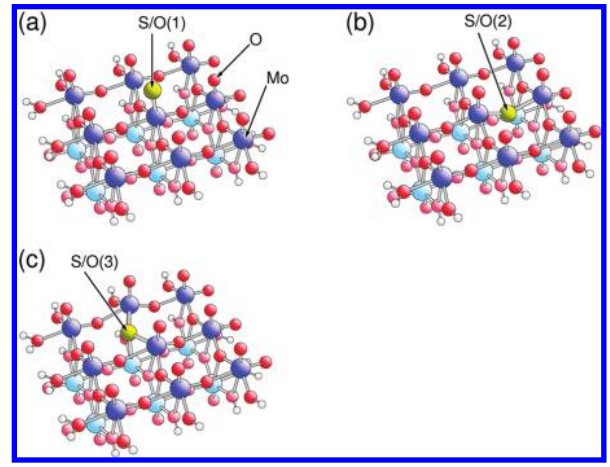


**Figure 2.** Equilibrium geometry of substitutional sulfur at different oxygen sites of the perfect $MoO_3(010)$ surface; see text. Sulfur, molybdenum, oxygen, and saturator hydrogen atoms are shown by very large, large, small, and very small shaded balls, respectively. Sulfur substituting oxygen at (a) O(1), denoted S/O(1); (b) O(2), denoted S/O(2); and (c) O(3), denoted S/O(3).

The energetic order of $E_{sb}(O)$ may suggest that singly coordinated oxygen O(1) at the $MoO_3(010)$ surface participates preferentially in oxidation reactions, according to the Mars−van Krevelen mechanism.[26] However, the size of the energies $E_{sb}(O)$ shows clearly that removing oxygen from the surface without any concurrent reaction requires a large energy that may be difficult to obtain in a chemical reaction.

Table 1 contains also results for surface binding energies $E_{sb}(S)$ of substitutional sulfur replacing oxygen at O(1), O(2), or O(3) sites, according to definition 2. Here, corresponding sulfur-substituted substrate clusters $Mo_{15}O_{55}SH_{22}$ and their oxygen vacancy counterparts $Mo_{15}O_{55}H_{22}$ (vacancy clusters) are considered where, in both cases, calculated equilibrium geometries with respect to sulfur incorporation and oxygen vacancy formation are used; see Figure 2. In addition, atomic sulfur is taken as reference. The numerical $E_{sb}(S)$ results are found to be always smaller in absolute value compared with the corresponding $E_{sb}(O)$ values. This shows that sulfur−substrate binding is overall weaker than oxygen−substrate binding, which is consistent with all interatomic distances $d$(S−Mo) being larger than corresponding $d$(O−Mo) values. Further, substitutional sulfur is bound most strongly at an O(1) vacancy site, denoted S/O(1) in Figure 2a, where oxygen is bound the weakest; see above. This suggests that the initial step of sulfidation of the $MoO_3$ substrate takes place preferentially at the O(1) site, which is confirmed by the results for the oxygen-by-sulfur substitution energies $E_{S/O}$ with gas-phase $H_2O$ and $H_2S$ as references; see definition 3. The numerical data of Table 1 show a mildly exothermic substitution, $E_{S/O} = -0.15$ eV, for the O(1) site, whereas the energies for the other oxygen sites, 1.6−2.1 eV, yield strongly endothermic substitution.

During the sulfidation process, sulfur may also be deposited at the $MoO_3(010)$ surface and stabilize at different sites. Therefore, we consider the adsorption of atomic sulfur at the perfect $MoO_3(010)$ surface in cluster calculations, including adsorption-induced local relaxation illustrated in Figure 1 of the Supporting Information. The results of corresponding adsorption energies $E_{ads}(S)$ using $Mo_{15}O_{56}SH_{22}$ as the substrate cluster and gas-phase sulfur as reference (see definition 4, are listed in Table 2. Sulfur adsorption at the bridging O(3) sites of the $MoO_3(010)$ surface is found to result in a metastable state with a positive $E_{ads}$ value and will not be considered further. In

**TABLE 2: Adsorption Energies, $E_{ads}(S)$ and $E_{ads}(S)'$, of Sulfur and Surface Binding Energies, $E_{sb}(SO)$, at the Perfect $MoO_3(010)$ Surface for Different Oxygen Sites Obtained from Cluster Model Calculations; See Text. The Table Includes Equilibrium Distances, $d(S-O)$, between Surface Oxygen at the Corresponding Sites, O(1), O(2), and O(3), and Adsorbed Sulfur[a]**

| site | O(1) | O(2) | O(3) |
|---|---|---|---|
| $E_{ads}(S)$ | −1.24 | −0.22 | 0.30 |
| $E_{ads}(S)'$ | 1.84 | 2.86 | 3.38 |
| $d(S-O)$ | 1.68 | 1.67 | 1.77 |
| $E_{sb}(SO)$ | −1.25 | −0.53 | −0.80 |

[a] All energies are given in eV, distances in Å.

contrast, the sulfur adsorbate stabilizes above the oxygen sites O(1) and O(2) at the surface with adsorption energies $E_{ads}(S) = -1.24$ and $-0.22$ eV, respectively, where it forms a negatively charged SO species. The adsorption energies are smaller in absolute size compared with corresponding surface binding energies $E_{sb}(S)$ of sulfur stabilizing in O(1) and O(2) oxygen vacancies ($-3.38$ and $-1.37$ eV; see Table 1). Thus, sulfur prefers to bind in oxygen vacancies, rather, at the perfect $MoO_3(010)$ surface. If sulfur adsorption is considered in a reaction where a $H_2S$ molecule in gas phase provides the sulfur adsorbate and is reduced to gas-phase $H_2$, then the corresponding adsorption energy $E_{ads}(S)'$ is given by definition 10 and differs from $E_{ads}(S)$ of definition 4 by the energy of the gas-phase reaction $(H_2S)_{gas} \rightarrow (H_2)_{gas} + (S)_{gas}$, which yields 3.08 eV from the present calculations. This results in strongly positive $E_{ads}(S)'$ values, 1.8−3.4 eV (see Table 2), which suggest that, starting from gas-phase $H_2S$, the sulfur adsorption is quite endothermic. In fact, a comparison with corresponding oxygen-by-sulfur substitution energies $E_{S/O}$ of Table 1 shows that $E_{ads}(S)'$ lies always above $E_{S/O}$ for the same oxygen site. This can be interpreted as sulfur−oxygen exchange reactions being energetically preferred over sulfur adsorption at the $MoO_3(010)$ surface.

The SO species formed after sulfur adsorption above the surface oxygen sites, O(1), O(2), and O(3), is bound to the substrate overall more strongly than the sulfur adsorbate, as suggested by the surface binding energy values $E_{sb}(SO)$ (see definition 5) included in Table 2. However, the $E_{sb}(SO)$ values are considerably smaller than the corresponding surface binding energies $E_{sb}(O)$ of oxygen by itself. This indicates that removal of oxygen from the $MoO_3(010)$ surface is easier in the presence of the sulfur adsorbate, a result that is more general and has been found also for other adsorbates and oxides. As examples, we mention that oxygen vacancy formation at differently coordinated sites of the $V_2O_5(010)$ surface is facilitated by preadsorbed hydrogen or oxygen.[19]

***3.1.2. Binding at the Sulfidic $MoO_3(010)$ Surface.*** The importance of substitutional sulfur at the $MoO_3(010)$ surface is examined by first exchanging an oxygen at the O(1) site by sulfur, yielding a local model of the sulfidic surface. Oxygen surface binding as well as surface binding of a second substitutional sulfur at oxygen sites near the exchange site is then considered. The latter can also be viewed as substitution of oxygen at two adjacent surface sites by sulfur, as illustrated in Figure 3. The binding analysis is analogous to the procedure for the perfect $MoO_3(010)$ surface, except that now surface binding energies $E_{sb}(O)$ and $E_{sb}(S)$ (see definitions 1 and 2) refer to a substrate cluster Sub = $Mo_{15}O_{55}SH_{22}$ with substitutional sulfur at the central O(1) surface site. Table 3 lists corresponding surface binding energies for oxygen sites, O(1), O(2), and O(3), adjacent to the substitution site with atomic oxygen and sulfur

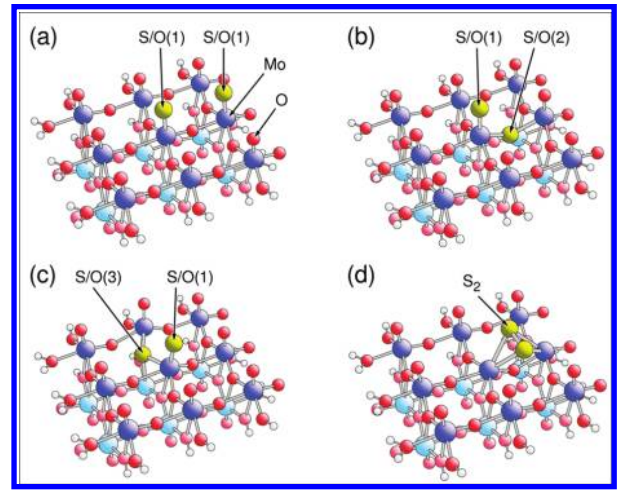


**Figure 3.** Equilibrium geometry of substitutional sulfur atoms at two adjacent oxygen sites of the perfect $MoO_3(010)$ surface (substitutional sulfur at the sulfidic $MoO_3(010)$ surface; see text). The different atoms are shown by shaded balls of different sizes; see the caption of Figure 2. Sulfur substituting oxygen at (a) adjacent O(1) sites, (b) adjacent O(1) and O(2) sites, and (c) adjacent O(1) and O(3) sites. (d) Geometric structure of molecular $S_2$ above the O(2) site.

**TABLE 3: Surface Binding Energies, $E_{sb}(X)$, X = O, S, at the Sulfidic $MoO_3(010)$ Surface for Different Oxygen Sites Obtained from Cluster Model Calculations; See Text. The Table Includes Equilibrium Distances $d(X-Mo)$ of the Two Species with Respect to Their Nearest Mo Neighbors at the Surface[b]**

| site | O(1) | O(2) | O(3) |
|---|---|---|---|
| $E_{sb}(O)$ | −5.53 | −5.84 | −6.35 |
| $d(O-Mo)$ | 1.69 | 1.75 | 1.95 |
| $E_{sb}(S)$ | −3.65 | −1.60 | −2.72 |
| $d(S-Mo)$ | 2.15 | 2.11 | 2.29 |
| $E_{S/O}$[a] | −0.25 | 2.10 | 1.49 |

[a] $E_{S/O}$ denotes oxygen/sulfur substitution energies; see text. [b] All energies are given in eV, distances in Å.

taken as reference. The $E_{sb}(O)$ results yield, for all sites, quite large and the $E_{sb}(S)$ data moderately large values, which indicates, as for the perfect $MoO_3(010)$ surface, rather strong surface binding of the two species. A comparison with Table 1 evidences that $E_{sb}(O)$ and $E_{sb}(S)$ variations due to substitutional sulfur are always below 0.2 eV. Thus, the presence of substitutional sulfur at the surface does not lead to major changes of the surface binding energies of nearby oxygen or sulfur, which suggests rather local binding of the two species at the surface.

Table 3 includes also results for the oxygen-by-sulfur substitution energies $E_{S/O}$ at oxygen sites near the exchange site. The numerical values are obtained using definition 3 with Sub = $Mo_{15}O_{55}SH_{22}$ and gas-phase $H_2O$ and $H_2S$ as references. A comparison with Table 1 shows that the calculated substitution energies for the sulfidic $MoO_3(010)$ surface are quite similar to those of the perfect surface, with differences for the oxygen sites, O(1), O(2), and O(3), being always below 0.1 eV. In particular, the general trend of a mildly exothermic substitution, $E_{S/O} = -0.25$ eV, for the O(1) site and strongly endothermic substitutions, $E_{S/O} = 2.10$ and 1.49 eV, for the O(2) and O(3) sites remains unchanged by the presence of the initial substituted sulfur, confirming the rather local binding of the two species. The $E_{S/O}$ results show further that the second sulfidation step after substituting oxygen at an O(1) site of the surface by sulfur takes place preferentially at another O(1) site where the two

sulfurs are well-separated and do not affect each other. However, it must be emphasized that these findings refer only to the initial sulfidation steps and may differ with increasing surface sulfidation.

Experimental studies on the sulfidation of $MoO_3$ catalysts have concluded that molecular ions $S_2^{-x}$ are formed as a consequence of the sulfidation process.[17,18] This has been examined in test calculations where the $MoO_3$(010) surface is modeled by a $Mo_{15}O_{54}H_{22}$ substrate cluster with two oxygen vacancies at adjacent O(1) sites and molecular $S_2$ added near these sites. After equilibration, the $S_2^{x-}$ surface species is found to stabilize between the two O(1) sites with its molecular axis perpendicular to the line between the sites, as shown in Figure 3d. The resulting surface binding energy defined by

$$E_{sb}(S_2)=E_{tot}(Mo_{15}O_{54}H_{22}S_2) - E_{tot}(Mo_{15}O_{54}H_{22}) - E_{tot}(S_2) \quad (11)$$

amounts to −0.49 eV, with an intramolecular distance, $d_{S-S}$ = 2.01 Å, which is larger than the gas-phase value of neutral $S_2$, 1.92 Å, reflecting the fact that the surface species is negatively charged.

***3.1.3. Binding at the Reduced $MoO_3$(010) Surface.*** When the $MoO_3$(010) surface is reduced by oxygen vacancies formed as a consequence of reactions or for thermodynamic reasons, its adsorption and reaction properties are expected to be influenced. This is examined by model calculations where, first, an oxygen vacancy at the (energetically preferred) O(1) site of the surface is formed; see Figure 2a of the Supporting Information. Oxygen surface binding as well as surface binding of a substitutional sulfur at oxygen sites near the vacancy site is then considered. Here, surface binding energies $E_{sb}$(O) and $E_{sb}$(S) (see definitions 1 and 2) refer to a substrate cluster, Sub = $Mo_{15}O_{55}H_{22}$, which includes an oxygen vacancy at the O(1) site near the center of the cluster surface. Thus, $E_{sb}$(O) for oxygen sites near the vacancy can be considered to describe also the energy required to form a second vacancy, where equilibrium geometries of different double oxygen vacancies, taken as references, are shown in Figure 2b−d of the Supporting Information.

Previous theoretical studies on oxygen vacancy formation at the $MoO_3$(010) surface based on the $Mo_{15}O_{55}H_{22}$ vacancy cluster have shown that geometric relaxation near an O(1) vacancy causes the adjacent asymmetrically bridging O(2) oxygen to move upward, forming a singly coordinated O(1)-type species, called O(1)′ in the following, with its Mo−O axis tilted with respect to that of the initial O(1) species.[19,27,28] This is confirmed by the present calculations (see Figure 2a of the Supporting Information) and may be the initial step of a major surface reconstruction due to reduction, which has also been considered in experimental studies.[29,30]

Table 4 contains surface binding energies $E_{sb}$(O) and $E_{sb}$(S) for oxygen sites, O(1), O(2), and O(3), adjacent to the O(1) vacancy site of the reduced $MoO_3$(010) surface, applying definitions 1 and 2, where Sub = $Mo_{15}O_{55}H_{22}$ and atomic oxygen and sulfur are taken as reference. Corresponding equilibrium geometries of substitutional sulfur adjacent to the O(1) vacancy site are sketched in Figure 3 of the Supporting Information. As for the perfect surface, the numerical $E_{sb}$(S) results for each site are smaller in absolute value compared with the corresponding $E_{sb}$(O) values, reflecting overall weaker sulfur−substrate compared with oxygen−substrate binding. However, all surface binding energies $E_{sb}$(O) and $E_{sb}$(S) for the reduced surface are larger in absolute value compared with those of the perfect surface. In addition, the energetic orders of $E_{sb}$(O) and $E_{sb}$(S) for different sites at the perfect surface are changed for the reduced surface. This is explained by the electronic influence of the vacancy at the reduced surface. First, the charge redistribution near the oxygen vacancy increases the binding ability of its nearby atom neighbors, thus, strengthening surface bonds and increasing the absolute $E_{sb}$ values. Second, the electronic charge distribution near the vacancy is strongly perturbed where the perturbation depends on the vacancy site, O(1), O(2), or O(3), and obviously leads to different energetic orders for the $E_{sb}$ data.

**TABLE 4: Surface Binding Energies, $E_{sb}$(X), X = O, S, at the Reduced $MoO_3$(010) Surface for Different Oxygen Sites Obtained from Cluster Model Calculations; See Text. The Table Includes Equilibrium Distances $d$(X−Mo) of the Two Species with Respect to Their Nearest Mo Neighbors at the Surface[b]**

| site | O(1) | O(2)/O(1)′ | O(3) |
|---|---|---|---|
| $E_{sb}$(O) | −6.61 | −6.97 | −6.22 |
| $d$(O−Mo) | 1.71 | 1.69 | 1.95 |
| $E_{sb}$(S) | −4.61 | −4.97 | −3.08 |
| $d$(S−Mo) | 2.14 | 2.12 | 2.21 |
| $E_{S/O}$[a] | −0.13 | −0.13 | 1.02 |

[a] $E_{S/O}$ denotes oxygen/sulfur substitution energies; see text. [b] All energies are given in eV, distances in Å.

The surface binding energies $E_{sb}$(O) (and $E_{sb}$(S)) for the oxygen sites O(1) and O(2) at the reduced surface are found to be rather similar. This can be understood by the surface relaxation induced by the O(1) vacancy (see above), which affects the O(2) oxygen most strongly and changes its electronic binding properties such that it becomes O(1)-type. The similarity is also reflected in the results for oxygen-by-sulfur substitution energies $E_{S/O}$ near a vacancy of the reduced surface (see definition 3), with Sub = $Mo_{15}O_{55}H_{22}$, including an oxygen vacancy at the O(1) site near the center of the cluster surface. The numerical $E_{S/O}$ values of Table 4 show a mildly exothermic substitution, $E_{S/O}$ = −0.13 eV, for both the O(1) and the O(2) site, comparable with the result for the O(1) site at the perfect surface, with stronger endothermic substitution, $E_{S/O}$ = 1.02 eV, for the O(3) site.

**3.2. Hydrogen Adsorption at the $MoO_3$(010) Surface.** In the experiment, the sulfidation of $MoO_3$ is achieved by exposing the substrate to a mixture of $H_2S$ and $H_2$ gas. Therefore, it is important to consider also hydrogen adsorption at the substrate surface in a proper description of the sulfidation process. This will be discussed in the following.

***3.2.1. Hydrogen Adsorption at the Perfect $MoO_3$(010) Surface.*** First, we examine the adsorption of atomic hydrogen at the perfect $MoO_3$(010) surface in cluster calculations, including adsorption-induced local relaxation illustrated in Figure 4, which sketches calculated adsorbate equilibrium geometries. Table 5a lists results of corresponding energies $E_{ads}$(H) of single-atom adsorption near different oxygen sites, O(1), O(2), and O(3), of the perfect $MoO_3$(010) surface; see definition 4, with Sub = $Mo_{15}O_{56}H_{22}$ and Ad = H. The numerical data for $E_{ads}$(H) evidence that hydrogen stabilizes at all three oxygen sites, forming rather strong bonds with the substrate oxygen where binding is the strongest at the asymmetric bridging O(2) site. This is slightly different from results from earlier calculations[19] that yield overall adsorption energies of smaller absolute size (differences ranging between 0.4 and 1.0 eV) and suggests that the O(1) site is energetically preferred. The differences are found to be due to different geometric relaxation where the atom environment near the adsorption site

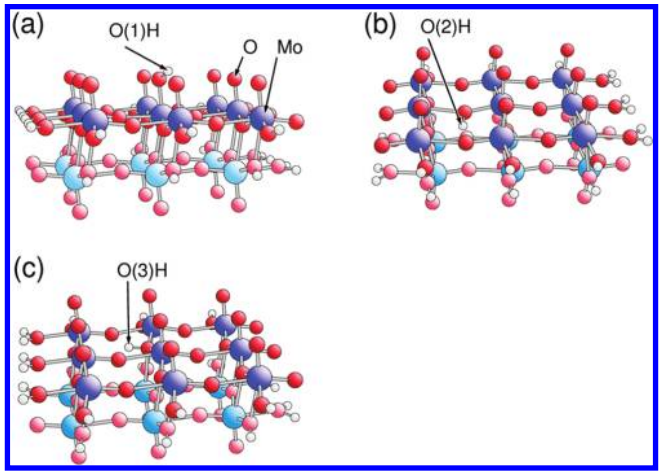


**Figure 4.** Equilibrium geometry of single hydrogen atoms adsorbed at different oxygen sites of the perfect $MoO_3(010)$ surface and forming OH groups; see text. The different atoms are shown by shaded balls of different sizes; see the caption of Figure 2. Hydrogen (a) adsorbed at O(1), forming O(1)H; (b) adsorbed at O(2), forming O(2)H; and (c) adsorbed at O(3), forming O(3)H.

**TABLE 5: Adsorption Energies of Hydrogen and Surface Binding Energies of Surface OH and $H_2O$ for Different Oxygen Sites, O(1), O(2), and O(3), at the Perfect $MoO_3(010)$ Surface Obtained from Cluster Model Calculations. The Table Includes Equilibrium Distances, $d$(O−H), between Surface Oxygen and Adsorbed Hydrogen as Well as Distances, $d$(O−Mo), between Oxygen and Neighboring Molybdenum[a,b]**

(a) adsorption of a single hydrogen

| site | O(1) | O(2) | O(3) |
|---|---|---|---|
| $E_{ads}$(H) | −2.08 | −2.48 | −1.74 |
| $d$(O−H) | 0.98 | 0.99 | 0.99 |
| $d$(O−Mo) | 1.87 (1.70) | 1.97 (1.75) | 2.08 (1.95) |
| $E_{sb}$(OH) | −2.86 | −3.56 | −3.62 |

(b) adsorption of two hydrogen atoms at the same oxygen site

| site | O(1) | O(2) | O(3) |
|---|---|---|---|
| $E_{ads}$(2H) | −4.55 | −4.61 | − |
| $d$(O−H) | 0.99, 0.98 | 1.00, 1.00 | − |
| $d$(O−Mo) | 2.20 (1.70) | 2.17 (1.75) | − |
| $E_{sb}$($H_2O$) | −0.13 | −0.48 | − |

(c) adsorption of two hydrogen atoms at adjacent oxygen sites

| site | O(1)/O(1) | O(1)/O(2) | O(1)/O(3) |
|---|---|---|---|
| $E_{ads}$(2H) | −4.04 | −4.22 | −3.75 |
| $d$(O−H) | 0.98/0.98 | 0.99/0.99 | 0.98/1.00 |
| $d$(O−Mo) | 1.88/1.88 | 1.83/1.98 | 1.89/2.05 |

[a] For definitions of $E_{ads}$(H), $E_{ads}$(2H), $E_{sb}$(OH), and $E_{sb}$($H_2O$), see text. All values are obtained from cluster model calculations using $Mo_{15}O_{56}H_{22}$ as the surface cluster. [b] The numbers in parentheses refer to the surface without adsorbate. All energies are given in eV, distances in Å.

allowed to relax in response to the adsorbate was chosen larger in the present than in the earlier calculations. It should be noted that the present adsorption energies $E_{ads}$(H) refer to atomic hydrogen in gas phase as a reference. The use of molecular $H_2$ as reference would decrease all absolute values of $E_{ads}$(H) by $^1/_2E_D(H_2)$, where $E_D(H_2)$ is the dissociation energy of gas-phase $H_2$, yielding 4.57 eV in the present calculations.

Hydrogen adsorption results in negatively charged OH groups at the substrate surface, which themselves are more weakly bound to the substrate than the initial oxygen species. This becomes evident from a comparison of the OH surface binding data $E_{sb}$(OH) of Table 5a (evaluated according to definition 6) with corresponding values $E_{sb}$(O) for the perfect $MoO_3(010)$ surface (see Table 1), which yield, for all oxygen sites, absolute values $|E_{sb}(OH)|$ smaller than $|E_{sb}(O)|$. The weakening of the oxygen−substrate bond due to the presence of adsorbed hydrogen is confirmed further by increased interatomic distances $d$(O−Mo), as evident from the $d$(O−Mo) values of Table 5a. For all oxygen sites, the resulting OH groups are strongly tilted with respect to the surface normal direction and lie almost flat at the surface; see Figure 4. These geometries are different from the equilibrium geometries determined previously in which OH was pointing perpendicular to the surface.[19] The discrepancy is explained, as before, by incomplete atom relaxation in the previous study.

Adsorbed hydrogen may desorb from the perfect $MoO_3(010)$ surface where two scenarios can be considered. In a direct process, the hydrogen atom leaves the surface, where the energy required for desorption equals the energy $|E_{ads}(H)|$ gained by adsorption. Alternatively, the surface OH group formed by adsorption may desorb as a whole, leaving a surface vacancy behind. The corresponding desorption energy equals the surface binding energy $|E_{sb}(OH)|$. Table 5a shows that the quantities $|E_{sb}(OH)|$ are, for all oxygen sites, larger than the corresponding hydrogen adsorption energies $|E_{ads}(H)|$, which indicates that direct hydrogen desorption is always energetically preferable over OH desorption. On the other hand, the relation $|E_{sb}(OH)| < |E_{sb}(O)|$ discussed above suggests that the presence of preadsorbed hydrogen facilitates oxygen removal from the $MoO_3(010)$ surface, which is in qualitative agreement with earlier findings.[19]

Hydrogen adsorption at the $MoO_3(010)$ surface may also lead to two hydrogen atoms stabilizing at the same oxygen site of the surface, yielding surface water groups illustrated in Figure 5a,b, which sketches calculated equilibrium geometries of the adsorbate. Table 5b lists results of corresponding adsorption energies $E_{ads}$(2H) for the oxygen sites, O(1) and O(2); see definition 4, with Sub = $Mo_{15}O_{56}H_{22}$ and Ad = 2H. (The O(3) site is found to be unable to accommodate two hydrogen atoms and will not be considered in the following.) The numerical data of $E_{ads}$(2H) in Table 5b are found to be quite similar, −4.6 eV, for the two oxygen sites and amount to about twice the energies $E_{ads}$(H) for single hydrogen adsorption. This shows that two hydrogen atoms can stabilize at O(1) and O(2) sites, forming local $H_2O$ groups at the substrate surface. The surface $H_2O$ is much more weakly bound to the substrate than the initial oxygen species. In fact, surface $H_2O$ is even more weakly bound than surface OH. This is obvious from a comparison of the $H_2O$ surface binding data $E_{sb}(H_2O)$ of Table 5b (evaluated according to definition 7) with corresponding values $E_{sb}$(O) and $E_{sb}$(OH) (see Tables 1 and 5a), which always yield $|E_{sb}(H_2O)| < |E_{sb}(OH)| < |E_{sb}(O)|$. The increased weakening of the oxygen−substrate bond due to the presence of the two adsorbed hydrogen atoms is consistent with the increased interatomic distances, $d$(O−Mo), included in Table 5b, which are larger than for single hydrogen adsorption.

Analogous to the single hydrogen case, the two hydrogen atoms adsorbed at a common oxygen site may desorb from the $MoO_3(010)$ surface where different scenarios are possible. The two hydrogen atoms may leave the surface (simultaneously or subsequently), ending up as separate gas phase atoms, where the energy required for desorption equals the energy $|E_{ads}(2H)|$ gained by adsorption. In another scenario, the surface $H_2O$ species formed by adsorption may desorb as a whole, leaving a surface vacancy behind. The corresponding desorption energy then equals the surface binding energy $|E_{sb}(H_2O)|$. Table 5b

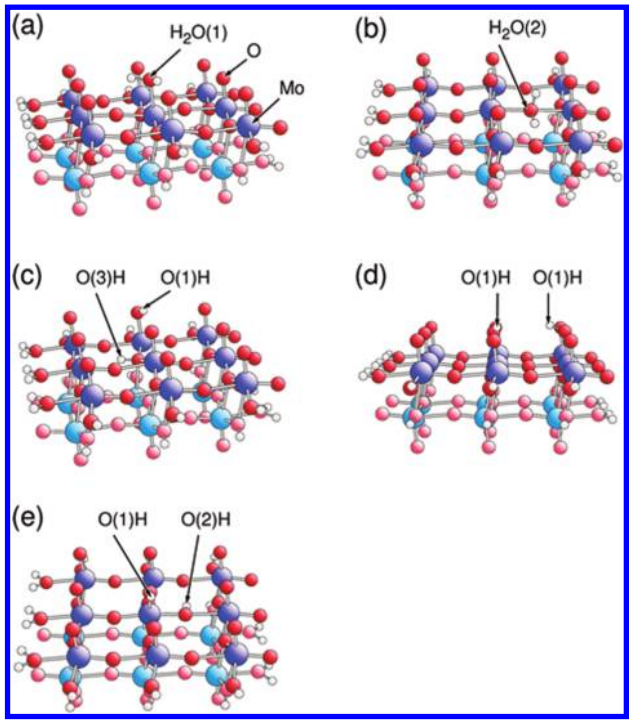


**Figure 5.** Equilibrium geometry of two hydrogen atoms adsorbed at different oxygen sites of the perfect $MoO_3(010)$ surface and forming $H_2O$ or adjacent OH groups; see text. The different atoms are shown by shaded balls of different sizes; see the caption of Figure 2. Two hydrogen atoms (a) adsorbed at O(1), forming $H_2O(1)$; (b) adsorbed at O(2), forming $H_2O(2)$; (c) stabilizing near O(3), forming an O(3)H and O(1)H pair; (d) adsorbed at adjacent O(1) sites, forming two O(1)H groups; and (e) adsorbed at adjacent O(1) and O(2) sites, forming an O(1)H and O(2)H pair.

shows that the quantities $|E_{sb}(H_2O)|$ are, for the two oxygen sites O(1) and O(2), substantially smaller than the corresponding hydrogen adsorption energies $|E_{ads}(2H)|$, which indicates that $H_2O$ desorption is energetically preferred over direct hydrogen desorption. In addition, the $|E_{sb}(H_2O)|$ values are considerably smaller compared with the corresponding surface binding (or vacancy formation) energies $|E_b(O)|$ of oxygen given in Table 1. This suggests, analogous to the results for surface OH groups discussed above, that the presence of preadsorbed hydrogen facilitates oxygen removal from the $MoO_3(010)$ surface where the effect is found to be stronger for surface $H_2O$ than for surface OH.

The electronic and energetic coupling between hydrogen atoms adsorbed at different oxygen sites of the $MoO_3(010)$ surface is examined in cluster model calculations where, in addition to adsorbing hydrogen at the O(1) site, a second hydrogen atom is stabilized at an adjacent O(1), O(2), or O(3) site. Table 5c lists results of adsorption energies $E_{ads}(2H)$ for two hydrogen atoms stabilizing at O(1)/O(1), O(1)/O(2), and O(1)/O(3) site pairs; see definition 4, with Sub = $Mo_{15}O_{56}H_{22}$ and Ad = 2H. (Corresponding equilibrium geometries are illustrated in Figure 5c−e.) These results can be compared with adsorption energies for two separated single hydrogen atoms listed in Table 5a in order to estimate the adsorbate−adsorbate interaction of hydrogen at adjacent oxygen sites. The comparison shows that, for O(1)/O(2) pairs, the $E_{ads}(2H)$ value, −4.22 eV, differs by 0.34 eV from the sum of the two energies $E_{ads}(H)$ for separate O(1) and O(2) sites, −4.56 eV. This suggests that the two adjacent adsorbates experience weak repulsion at the surface where, however, the effect is reasonably small. The interaction seems even smaller for the O(1)/O(1) and O(1)/O(3) pairs, where the difference between $E_{ads}(2H)$ and the sum of the two corresponding $E_{ads}(H)$ values amount to 0.12 and 0.07 eV, respectively. Altogether, the comparison indicates that hydrogen adsorption at the perfect $MoO_3(010)$ surface is a rather local process with little electronic coupling between neighboring adsorbates.

**TABLE 6: Adsorption Energies of Hydrogen Atoms and Surface Binding Energies of Surface OH for Oxygen Sites, O(1), O(2), and O(3), near a Sulfur Site at O(1) of the Sulfidic $MoO_3(010)$ Surface Obtained from Cluster Model Calculations. The Table Includes Equilibrium Distances, $d$(O−H), between Surface Oxygen and Adsorbed Hydrogen as Well as Distances, $d$(O−Mo), between Oxygen and Neighboring Molybdenum[a,b]**

| site | O(1) | O(2) | O(3) |
|---|---|---|---|
| $E_{ads}(H)$ | −2.11 | −2.35 | −1.69 |
| $d$(O−H) | 0.98 | 0.99 | 0.99 |
| $d$(O−Mo) | 1.88 (1.69) | 1.98 (1.75) | 2.08 (1.95) |
| $E_{sb}(OH)$ | −3.07 | −3.62 | −3.46 |

[a] For definitions of $E_{ads}(H)$ and $E_{sb}(OH)$, see text. [b] The numbers in parentheses refer to the sulfidic surface without adsorbate; see Table 3. All energies are given in eV, distances in Å.

***3.2.2. Hydrogen Adsorption at the Sulfidic $MoO_3(010)$ Surface.*** Hydrogen will also be present at the sulfidic $MoO_3$ surface where different scenarios are conceivable. First, hydrogen may adsorb at oxygen sites of the surface that are further away from sulfur sites. This scenario is included in the treatment of adsorption at the perfect surface discussed in section 3.2.1. Second, atomic hydrogen may stabilize at different oxygen sites adjacent to substitutional sulfur at the $MoO_3(010)$ surface. Third, atomic hydrogen may adsorb directly at the different substitutional surface sulfur sites.

The second scenario is accounted for by, first, exchanging oxygen at the O(1) site by sulfur, yielding a local model of the sulfidic surface. Hydrogen adsorption at oxygen sites near the exchange site is then considered. The binding analysis is analogous to the procedure for the perfect $MoO_3(010)$ surface described in section 3.2.1, except that, now, adsorption energies $E_{ads}(H)$ (see definition 4) refer to a substrate cluster, Sub = $Mo_{15}O_{55}SH_{22}$, with substitutional sulfur at the central O(1) surface site. Table 6 lists results of corresponding energies $E_{ads}(H)$ of single hydrogen adsorption near oxygen sites, O(1), O(2), and O(3), of the sulfidic $MoO_3(010)$ surface where atomic hydrogen is used as the gas-phase reference. These data can be compared with results for the perfect surface given in Table 5a. The comparison shows that the adsorption energy $E_{ads}(H)$ for the O(1) site is slightly more negative, by 0.03 eV, for the sulfidic than for the perfect surface, whereas it is less negative, by 0.13 and 0.05 eV, for the O(2) and O(3) sites. This suggests increased adsorptive H−O binding at the O(1) site due to the presence of nearby sulfur, whereas binding seems to be weakened by sulfur at the O(2) and O(3) sites. The different behavior may be explained by geometric effects because the distance between the hydrogen adsorbate and the substitutional sulfur is larger for adsorption at O(1) compared with O(2) and O(3). However, the energetic influence is always rather small for the present model, which is confirmed by the interatomic distances, $d$(O−H) and $d$(O−Mo), differing very little between adsorption at the perfect and sulfidic surfaces. In fact, total equilibrium geometries for hydrogen adsorption at the sulfidic surface clusters differ only marginally from those of the perfect surface clusters (see Figure 4) and are, therefore, not shown separately. However, the influence of substitutional sulfur for

**TABLE 7: Adsorption Energies of Hydrogen and Surface Binding Energies of Surface SH and $H_2S$ for Sulfur Substituting Different Oxygen Sites of the Sulfidic $MoO_3$(010) Surface Obtained from Cluster Model Calculations, See Text. The Table Includes Equilibrium Distances, $d$(S−H), between Surface Sulfur and Adsorbed Hydrogen as Well as Distances, $d$(S−Mo), between Sulfur and Neighboring Molybdenum[a,b]**

(a) adsorption of a single hydrogen atom

| site | S/O(1) | S/O(2) | S/O(3) |
|---|---|---|---|
| $E_{ads}$(H) | −2.12 | −2.28 | −2.22 |
| $d$(S−H) | 1.38 | 1.37 | 1.38 |
| $d$(S−Mo) | 2.31 (2.15) | 2.24 (2.11) | 2.48 (2.29) |
| $E_{sb}$(SH) | −1.82 | 0.03 | −1.29 |

(b) adsorption of two hydrogen atoms at the same sulfur site

| site | S/O(1) | S/O(2) | S/O(3) |
|---|---|---|---|
| $E_{ads}$(2H) | −4.47 | −4.05 | − |
| $d$(S−H) | 1.38, 1.37 | 1.39, 1.40 | − |
| $d$(S−Mo) | 2.49 (2.15) | 2.28 (2.11) | − |
| $E_{sb}$($H_2S$) | −0.20 | 2.22 | − |

[a] The substitution sites at O(1), O(2), and O(3) sites are termed S/O(1), S/O(2), and S/O(3). For definitions of $E_{ads}$(H), $E_{ads}$(2H), $E_{sb}$(SH), and $E_{sb}$($H_2S$), see text. [b] The numbers in parentheses refer to the sulfidic surface without adsorbate; see Table 3). All energies are given in eV, distances in Å.

hydrogen adsorption is expected to become more important for higher sulfur concentration at the surface.

The third scenario describing hydrogen adsorption directly at substitutional sulfur sites starts from exchanging oxygen at different surface sites by sulfur to yield a local model of the sulfidic surface. Hydrogen adsorption at the sulfur sites is then considered. Table 7a lists numerical data of corresponding adsorption energies $E_{ads}$(H), referring to substitutional sulfur sites at O(1), O(2), and O(3) sites of the sulfidic $MoO_3$(010) surface, where definition 4, with Sub = $Mo_{15}O_{55}SH_{22}$ and Ad = H, is applied and equilibrium geometries are sketched in Figure 4 of the Supporting Information. In the following, these sulfur adsorption sites will be termed S/O($i$) for S at O($i$), $i$ = 1, 2, 3. The results for $E_{ads}$(H) confirm that hydrogen stabilizes at all sulfur sites, forming rather strong bonds with the sulfur where binding is the strongest with sulfur at the asymmetric bridging O(2) site, analogous to the surface oxygen case of section 3.2.1. However, the $E_{ads}$(H) values cover a much smaller energy range, −2.1 to −2.3 eV, as compared with those for the perfect surface, −1.7 to −2.5 eV. This can be understood by the fact that sulfur itself stabilizes at larger distances $d$(S−Mo) with respect to neighboring Mo atoms of the substrate compared with corresponding $d$(O−Mo) values for oxygen and is more weakly bound to the $MoO_3$ substrate than surface oxygen; see the data of Table 3. Thus, hydrogen adsorption at sulfur sites is influenced less by site-dependent geometric details of the surface compared with adsorption at corresponding oxygen sites.

Hydrogen adsorption at sulfur sites leads to negatively charged SH groups at the substrate surface with properties that can be compared with those found for OH groups at the perfect $MoO_3$(010) surface. Analogous to OH, the SH groups are much more weakly bound to the substrate than the initial sulfur species, as shown by a comparison of the $E_{sb}$(SH) values of Table 7a with $E_{sb}$(S) values of Table 1, yielding roughly $E_{sb}$(SH) = $E_{sb}$(S) + 1.5 eV. This leads to positive $E_{sb}$(SH) for the O(2) site, making SH a metastable surface species. Interestingly, the geometric effect of hydrogen binding to surface sulfur is smaller than for surface oxygen. The increase in distance $d$(S−Mo) due to hydrogen amounts to 0.03−0.19 Å (see Table 7a), while the corresponding $d$(O−Mo) distance increase yields 0.13−0.22 Å. This difference may be explained by sulfur itself stabilizing further away from neighboring molybdenum compared with oxygen such that hydrogen adsorption has a smaller influence on S−Mo than on O−Mo binding. A comparison of Figures 4 and 4 of the Supporting Information, sketching the equilibrium geometries of OH and SH groups at different oxygen sites of the $MoO_3$(010) surface, shows overall rather similar geometries (with minor distance and angle changes) for the S/O(1) and S/O(2) sites. In contrast, the SH group stabilizing near the S/O(3) site is pushed outward while the oxygen of OH at this site remains near its position at the perfect surface. This difference is due to the increased size of sulfur compared with oxygen, which yields larger steric repulsion—the sulfur does not fit into the O(3) vacancy—as is already evident from the equilibrium geometry of substitutional sulfur at the O(3) site shown in Figure 2c.

Adsorbed hydrogen may desorb from the sulfidic $MoO_3$(010) surface where, apart from direct desorption requiring $|E_{ads}(H)|$ gained by adsorption, the surface SH group formed by adsorption may desorb as a whole, leaving a surface vacancy behind. Here, desorption requires the surface binding energy $|E_{sb}(SH)|$. Table 7a shows that the quantities $|E_{sb}(SH)|$ are, for all oxygen sites, smaller than the corresponding hydrogen adsorption energies $|E_{ads}(H)|$. This suggests that direct hydrogen desorption is energetically less preferable compared with SH desorption, in contrast to the results for H and OH desorption at the perfect surface. Further, the $|E_{sb}(SH)|$ values are considerably smaller compared with the corresponding surface binding energies $|E_b(S)|$ of sulfur; see Table 1. This suggests that the presence of preadsorbed hydrogen facilitates sulfur removal from the sulfidic $MoO_3$(010) surface, as found already for oxygen.

The adsorption of two hydrogen atoms may occur at the same sulfur site of the surface, yielding negatively charged surface $H_2S$ groups. Table 7b lists results of corresponding adsorption energies $E_{ads}$(2H) for two hydrogen atoms stabilizing at the same sulfur site, S/O(1) and S/O(2), of the sulfidic $MoO_3$(010) surface (see definition 4, with Sub = $Mo_{15}O_{55}SH_{22}$ and Ad = 2H), illustrated in Figure 5a,b of the Supporting Information sketching calculated adsorbate equilibrium geometries. (The S/O(3) site is found to be unable to bind two hydrogen atoms. Approaching the two atoms near the S/O(3) site results in separate O(1)H and S(3)H groups adjacent to each other (see Figure 5c of the Supporting Information), which will not be considered further.) The numerical data of $E_{ads}$(2H) in Table 7b show that, for S/O(1), the adsorption energy $|E_{ads}(2H)|$ is larger than twice the value $|E_{ads}(H)|$ for single hydrogen adsorption. This means that the formation of local surface $H_2S$ groups at S/O(1) is energetically preferred over SH groups. In addition, the $H_2S$ groups are bound very weakly to the substrate, as evidenced by the surface binding data $E_{sb}$($H_2S$) of Table 7b (evaluated according to definition 9). Adsorption of two hydrogen atoms at a S/O(2) site yields $|E_{ads}(2H)|$ smaller than twice the corresponding value $|E_{ads}(H)|$. Thus, local surface SH groups at S/O(2) are energetically preferred over $H_2S$ groups. In fact, the $H_2S$ groups at S/O(2) are found to be strongly metastable, $E_{sb}$($H_2S$) > 0 (see Table 7b), and may not occur at the real surface. Altogether, analogous to the results for oxygen at the perfect $MoO_3$ surface, the presence of preadsorbed hydrogen facilitates also sulfur removal from the sulfidic $MoO_3$(010) surface.

**3.3. Reaction Steps of the Sulfidation of $MoO_3$.** The present cluster results can shed some light on possible reaction schemes for the catalytic sulfidation at the surface of $MoO_3$ substrate. The basic Mars−van Krevelen-type process may be viewed as

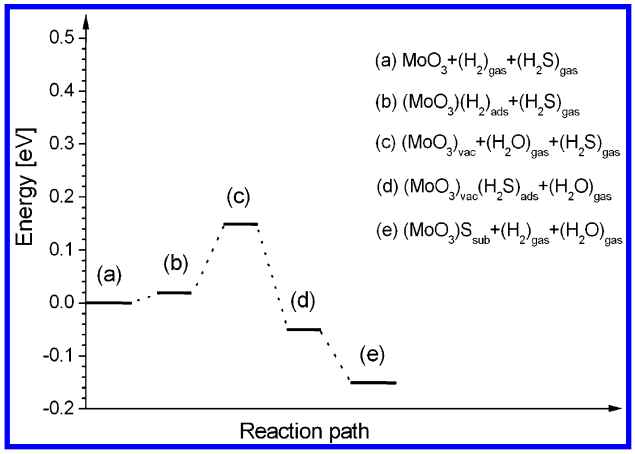


**Figure 6.** Energetics of the $MoO_3$ sulfidation with gas-phase hydrogen participating. Relative energies of the different product compositions a1−e1 along the reaction path (see text) are taken from cluster model calculations using $Mo_{15}O_{56}H_{22}$ as the basic surface cluster. The compositions a1−e1 discussed in the text are described to the right of the reaction scheme.

$H_2S$ approaching the oxide substrate and $H_2O$ leaving with one surface oxygen species being replaced by sulfur. Here, different reaction scenarios can be conceived that may or may not involve additional hydrogen from the gas phase, as proposed in the literature.[15,18] A first possible scenario where gas-phase hydrogen participates is described conceptionally by reaction steps between product compositions a1 and e1 as follows

$$MoO_3 + (H_2)_{gas} + (H_2S)_{gas} \quad \text{(a1)}$$

$$\rightarrow (MoO_3)(H_2)_{ads} + (H_2S)_{gas} \quad \text{(b1)}$$

$$\rightarrow (MoO_3)_{vac} + (H_2O)_{gas} + (H_2S)_{gas} \quad \text{(c1)}$$

$$\rightarrow (MoO_3)_{vac}(H_2S)_{ads} + (H_2O)_{gas} \quad \text{(d1)}$$

$$\rightarrow (MoO_3)S_{sub} + (H_2)_{gas} + (H_2O)_{gas} \quad \text{(e1)}$$

Figure 6 shows the energetics of this reaction scenario based on the present cluster model calculations, where it is assumed that the reaction site oxygen is singly coordinated O(1) at the $MoO_3$(010) surface. Relative energies of the different product compositions a1−e1 along the reaction path are obtained from the cluster total energies discussed in sections 3.1 and 3.2. Starting from the $MoO_3$ substrate and gas-phase $H_2$ and $H_2S$, composition a1, the first reaction step, from (a1) to (b1), is described by adsorbing gas-phase $H_2$ where the two hydrogen atoms stabilize at a surface oxygen site to yield a surface $H_2O$ group. This reaction step requires separating the two hydrogen atoms of molecular $H_2$, followed by adsorption at the surface oxygen site where further details depend on specific reaction paths and cannot be derived from the present calculations. However, the energy balance of this reaction step can be obtained by a model path considering the dissociation of molecular $H_2$ in the gas phase, which requires the dissociation energy, $E_D(H_2) = 4.57$ eV, from the present calculations, followed by adsorbing the two H atoms at the surface oxygen site. Assuming O(1) as the adsorption site, the cluster calculations yield an energy gain of 4.55 eV. This results in a combined energy cost of 0.02 eV for step (a1) to (b1). In the subsequent step, from (b1) to (c1), the surface $H_2O$ group desorbs into the gas phase, leaving an oxygen vacancy behind. This requires a desorption energy of 0.13 eV, calculated for the desorption from the O(1) site. In the next step, from (c1) to (d1), gas-phase $H_2S$ stabilizes in the oxygen vacancy at the $MoO_3$ surface, which can also be considered as two hydrogen atoms adsorbed at a substitutional sulfur site. On the basis of sulfur positioned at the O(1) site, this stabilization gains 0.20 eV from the present calculations. In the final step, from (d1) to (e1), the two hydrogen atoms binding to substitutional sulfur desorb into the gas phase, forming molecular $H_2$ and leaving substitutional sulfur at the substrate surface. In analogy with step (a1) to (b1), this final step combines hydrogen desorption with $H_2$ creation, where details depend on specific reaction paths and cannot be obtained by the present calculations. However, its energy balance can be determined by a model path where the two hydrogen species at the sulfur site desorb from the surface, yielding gas-phase atoms, which requires a desorption energy of 4.47 eV, calculated for the $H_2S$ group at an O(1) site, followed by combining the H atoms to molecular $H_2$ in gas phase, which gains the dissociation energy of 4.57 eV. This leads to a combined energy gain of 0.10 eV for the final step, from (d1) to (e1). Altogether, the net reaction energy for the complete path amounts to −0.15 eV, which indicates a slightly exothermic sulfidation process.

Obviously, the present reaction scenario involving gas-phase hydrogen is characterized by rather small energy differences, below 0.2 eV, between the product compositions a1−e1, which makes the reaction scheme thermodynamically attractive. However, the actual probability of the reaction scheme has to be estimated using also energetic details of all reaction paths where activation barriers can become important. Here, the two paths involving transitions between atomic and molecular hydrogen, from (a1) to (b1) and (d1) to (e1), are of particular interest. Although the energy balance of these reaction steps can be obtained from model paths involving hydrogen dissociation or recombination in the gas phase, these model paths with reaction barriers corresponding to the dissociation energy, $E_D(H_2) = 4.57$ eV, will not be realistic. Hydrogen dissociation/recombination is expected to happen near the $MoO_3$ substrate surface and may involve other surface atoms, which will result in much lower reaction barriers compared with $E_D(H_2)$. A quantitative account of more realistic barriers requiring studies of many alternative reaction paths is out of reach for the present work. In contrast, the other two steps, from (b1) to (c1) and (c1) to (d1), are very likely to come with only small or no activation barriers.

Alternative scenarios of the catalytic sulfidation include reactions where gas phase hydrogen does not participate. A first possible scheme is described conceptionally by reaction steps between compositions a2 and d2 as follows

$$MoO_3 + (H_2S)_{gas} \quad \text{(a2)}$$

$$\rightarrow (MoO_3)_{vac} + O_{gas} + (H_2S)_{gas} \quad \text{(b2)}$$

$$\rightarrow (MoO_3)_{vac} + S_{gas} + (H_2O)_{gas} \quad \text{(c2)}$$

$$\rightarrow (MoO_3)S_{sub} + (H_2O)_{gas} \quad \text{(d2)}$$

Starting from the $MoO_3$ substrate and gas-phase $H_2S$, composition a2, the first reaction step, from (a2) to (b2), is described by desorbing atomic oxygen and creating an oxygen vacancy

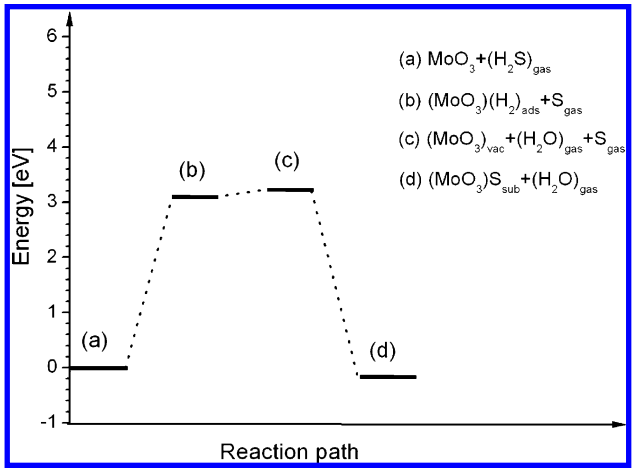


**Figure 7.** Energetics of the $MoO_3$ sulfidation without gas-phase hydrogen. Relative energies of the different product compositions a3−d3 along the reaction paths (see text) are taken from cluster model calculations using $Mo_{15}O_{56}H_{22}$ as the basic surface cluster. The compositions a3−d3 discussed in the text are described to the right of the reaction schemes.

at the substrate surface. Assuming O(1) as the surface oxygen site, the cluster calculations yield an energy cost of 5.36 eV. This energy is much too high to make the mechanism likely to happen. Therefore, it will not be pursued any further.

Another alternative scenario of the catalytic sulfidation where gas phase hydrogen does not participate is described conceptionally by a set of reaction steps between compositions a3 and d3 as follows

$$MoO_3 + (H_2S)_{gas} \quad \text{(a3)}$$

$$\rightarrow (MoO_3)(H_2)_{ads} + S_{gas} \quad \text{(b3)}$$

$$\rightarrow (MoO_3)_{vac} + (H_2O)_{gas} + S_{gas} \quad \text{(c3)}$$

$$\rightarrow (MoO_3)S_{sub} + (H_2O)_{gas} \quad \text{(d3)}$$

Figure 7 shows the energetics of this scheme based on the present cluster model calculations, again, with singly coordinated O(1) assumed as reaction site oxygen. Starting from the $MoO_3$ substrate and gas-phase $H_2S$, composition a3, the first reaction step, from (a3) to (b3), is described by splitting off the hydrogen from gas-phase $H_2S$ and adsorbing the H atoms at a surface oxygen site to yield a surface $H_2O$ group. For O(1) as the surface oxygen site, the cluster calculations yield an energy cost of 3.10 eV; see Figure 7. Again, details of the hydrogen separation from $H_2S$ in the gas phase depend on specific reaction paths that have not been considered. In the subsequent step, from (b3) to (c3), the surface $H_2O$ group desorbs into the gas phase, leaving an oxygen vacancy behind. This requires a desorption energy of 0.13 eV, calculated for the desorption from O(1). In the final step, from (c3) to (d3), gas-phase sulfur adsorbs in the oxygen vacancy at the $MoO_3$ surface to form the substitutional species. This gains the surface binding energy of sulfur, amounting to 3.38 eV, as calculated for substitutional sulfur at the O(1) site, which yields again a net reaction energy for the complete path of −0.15 eV.

The comparison of the different sulfidation scenarios allows an estimate of their relative importance. The energetics of each sequence of intermediate products sketched in Figures 6 and 7 suggest clearly that sulfidation becomes thermodynamically more favorable if hydrogen participates in the reaction. For the corresponding scenario (see Figure 6), composition c1, with a maximum energy of all compositions, lies only 0.15 eV above the initial composition (a1). In contrast, this maximum energy amounts to 3.23 eV, composition (c3) in Figure 7, for the scenario that excludes hydrogen as a reaction partner. Thus, hydrogen is found to facilitate the sulfidation process based on thermodynamic arguments. However, relative probabilities of the different reaction scenarios depend also on kinetic details defined by specific reaction paths of each scenario and must include corresponding barrier energies. Because of the complexity of the present reactions, there is a multitude of possible reaction paths between the different compositions and corresponding optimized paths are rather difficult to determine. Therefore, a comparison of the three scenarios as to their kinetic probability must be based on further estimates. As discussed above, the first scenario with participating hydrogen, Figure 6, includes, in its first step, hydrogen dissociation, which requires the dissociation energy of 4.57 eV. This energy can be considered a very rough upper limit of all reaction barriers occurring for the corresponding scenario. The scenario where hydrogen does not participate, Figure 7, includes, in its first step, hydrogen splitting from $H_2S$ in the gas phase, which requires a dissociation energy of 7.65 eV from the present calculations. This energy is expected to be reduced if splitting occurs near the substrate surface. However, its value is very unlikely to go below the upper bound of the first scenario, 4.57 eV. Altogether, the comparison indicates that the first scenario is also preferred on the basis of kinetic considerations. Thus, sulfidation can be considered more favorable if hydrogen participates in the reaction than in the absence of hydrogen, based on thermodynamic and kinetic estimates.

## 4. Conclusions

The present theoretical cluster studies provide detailed information on sulfidation of the $MoO_3$ substrate where its (010) oriented surface is considered as a model. As a first result, the studies, applying large surface clusters together with DFT methods to evaluate electronic, structural, and energetic parameters, show that oxygen at all three sites, terminal O(1) and bridging O(2) and O(3), of the perfect $MoO_3$(010) surface is bound rather strongly to its substrate environment with binding energies of −5.4 to −6.5 eV. Thus, oxygen removal (vacancy formation) without additional atoms or molecules participating is quite difficult. Further, substitutional sulfur replacing oxygen at one of the three surface sites is also bound quite strongly. However, the corresponding binding energies, between −1.4 and −3.4 eV, suggest sulfur−substrate binding to be overall weaker than oxygen−substrate binding. This is consistent with all interatomic distances $d$(S−Mo) being larger than the corresponding $d$(O−Mo) values, reflecting also the size difference between the two atoms. A comparison of the results for the different oxygen sites shows that the binding energy at the molybdenyl site O(1) is smallest for oxygen, 5.4 eV, whereas it is largest for sulfur, 3.4 eV. This suggests that the initial step of sulfidation of the $MoO_3$ substrate takes place preferentially at the molybdenyl site O(1). Sulfur adsorbing at an oxygen site of the $MoO_3$(010) surface can also be compared with sulfur substitution at the same site. Starting from $H_2S$, the adsorption process is strongly endothermic for all oxygen sites, whereas oxygen-by-sulfur substitution is less endothermic for the O(2) and O(3) sites and even slightly exothermic for the O(1) site. This can be interpreted as sulfur−oxygen exchange reactions being energetically preferred over sulfur adsorption at the $MoO_3$(010) surface.

The binding of oxygen as well as sulfur near substitutional sulfur sites of the sulfidic $MoO_3$(010) surface, represented by

additional sulfur at an (energetically preferred) O(1) site, is found to be quite similar compared to the corresponding binding at the perfect surface, which suggests rather local binding of the two species. In addition, the calculations show that the second oxygen-by-sulfur substitution after substituting oxygen at an O(1) site of the surface by sulfur takes place preferentially at an adjacent O(1) site where the two sulfurs are well-separated and do not affect each other. The binding of oxygen as well as sulfur near oxygen vacancy sites of the reduced $MoO_3$(010) surface, represented by a vacancy at an O(1) site, turns out to be qualitatively similar compared to the corresponding binding at the perfect surface. The calculations show, as before, overall weaker sulfur−substrate compared with oxygen−substrate binding. However, surface binding energies of both oxygen and sulfur near the oxygen vacancy are found to be larger in absolute value compared with those of the perfect surface. This is explained by the charge redistribution near the oxygen vacancy, which increases the binding ability of its nearby atom neighbors and strengthens neighbor bonds. Thus, oxygen vacancies at the reduced surface can stabilize substitutional sulfur.

In the experiment, sulfidation of $MoO_3$ is performed in the presence of hydrogen such that hydrogen participating in the sulfidation process cannot be excluded and hydrogen adsorption needs to be considered in a proper description. Atomic hydrogen is found to stabilize at all three oxygen sites, forming rather strong bonds with the substrate oxygen where binding is the strongest at the asymmetric bridging O(2) site of the perfect $MoO_3$(010) surface. Two separate H atoms can also stabilize at the same oxygen site, O(1) or O(2), with sizable binding energies where, again, the O(2) site is slightly preferred over O(1). Further, adsorption of two hydrogen atoms at adjacent oxygen sites prefers O(1)/O(2) site pairs. In all cases, adsorption results in surface OH and $H_2O$ groups that are bound to their surface environment much more weakly than the corresponding oxygen itself. This indicates that the presence of preadsorbed hydrogen facilitates oxygen removal from the perfect $MoO_3$(010) surface, which is in qualitative agreement with earlier findings.

At the sulfidic $MoO_3$(010) surface, hydrogen adsorbing at oxygen near the substitutional sulfur site behaves quite similar to adsorption at the perfect surface with only small differences in binding energies and interatomic distances. This confirms the local nature of the adsorptive H−O bond. Further, hydrogen adsorption at sulfur sites of the sulfidic surface yields, for sulfur at the O(1) site, a quite similar binding energy compared to that of the corresponding oxygen site at the perfect surface, whereas the differences are larger for the O(2) and O(3) sites. This reflects not only differences between the local H−S and H−O binding but also geometric effects due to the increased size of sulfur compared with oxygen.

Combining all results obtained for oxygen, sulfur, and hydrogen at the $MoO_3$(010) surface, we have considered model scenarios for the sulfidation based on Mars−van Krevelen-type processes viewed as $H_2S$ approaching the oxide substrate and $H_2O$ leaving with one surface oxygen species being replaced by sulfur. As mentioned above, in experiment, sulfidation of $MoO_3$ is always performed in the presence of gas-phase hydrogen. However, details of its role in the sulfidation process remain unclear. Therefore, it is interesting to compare reaction scenarios where hydrogen participates in the sulfidation reaction with those where it acts only as a spectator molecule. The present studies suggest a scenario (see Figure 6) where hydrogen helps to remove oxygen from the surface. This scenario is found to be energetically favored over alternative schemes (see Figure 7) where hydrogen does not participate in the sulfidation reaction. Therefore, we conclude that, based on the present model calculations, hydrogen is expected to participate actively in the sulfidation of $MoO_3$, facilitating the reaction process. These findings can be substantiated further by examining more specific reaction paths and evaluating reaction barriers that have been only roughly estimated in the present work.

**Acknowledgment.** This work was partly supported by the National Natural Science Foundation of China, Nos. 20590363, 20876163, and 10979068, by the State Key Fundamental Research Program, No. 2007CB216401, and by the Deutsche Forschungsgemeinschaft (DFG) through its Collaborative Research Center Sfb 546, "Transition metal oxide aggregates". X.S. is grateful for a stipend of the Max-Planck Society and the Chinese Academy of Sciences Doctoral Promotion Program.

**Supporting Information Available:** Five additional figures. This material is available free of charge via the Internet at http://pubs.acs.org.

## References and Notes

(1) Delmon, B. In *Catalysts in Petroleum Refining-1989*; Trimm, D. L., Akashah, S., Absi-Halabi, M., Bishara, A., Eds.; Elsevier: Amsterdam, The Netherlands, 1990; pp 1−40.
(2) Murchison, C. B.; Conway, M. M.; Stevens, R. R.; Guarderer, G. J. *Proc. Int. Congr. Catal., 9th* **1988**, *2*, 626.
(3) Lee, J. S.; Kim, S.; Lee, K. H.; Nam, I.-S.; Chung, J. S.; Kim, Y. G.; Woo, H. C. *Appl. Catal., A* **1994**, *110*, 11.
(4) Delmon, B.; Froment, G. *Catal. Rev.−Sci. Eng.* **1996**, *38*, 69.
(5) Topsøe, H.; Clausen, B. S.; Franklin, F. E.; Massoth, E. In *Science and Technology in Catalysis: Hydrotreating Catalysis*; Abderson, J. R., Boudart, M., Eds.; Springer: Berlin, Germany, 1996.
(6) Startsev, A. N. *Catal. Rev.−Sci. Eng.* **1995**, *37*, 353.
(7) Startsev, A. N. *J. Mol. Catal. A* **2000**, *152*, 1.
(8) Schrader, G. L.; Cheng, C. P. *J. Catal.* **1983**, *80*, 369.
(9) Kolboe, S.; Amberg, C. H. *Can. J. Chem.* **1966**, *44*, 2623.
(10) de Beer, V. H. J.; van der Aalst, M. J. M.; Machiels, C. J.; Schuit, G. C. A. *J. Catal.* **1976**, *43*, 78.
(11) Gissy, H.; Bartsch, R.; Tanielian, C. *J. Catal.* **1980**, *65*, 150.
(12) Arnoldy, P.; Van den Heijkant, J. A. M.; De Bok, G. D.; Moulijn, J. A. *J. Catal.* **1985**, *92*, 35.
(13) Scheffer, B.; Arnoldy, P.; Moulijn, J. A. *J. Catal.* **1988**, *112*, 516.
(14) Schild, Ch.; Engweiler, J.; Nickl, J.; Baiker, A.; Hund, M.; Kilo, M.; Wokaun, A. *Catal. Lett.* **1994**, *25*, 179.
(15) de Jong, A. M.; Borg, H. J.; van IJzendoorn, L. J.; Soudant, V. G. F. M.; de Beer, V. H. J.; van Veen, J. A. R.; Niemantsverdriet, J. W. *J. Phys. Chem.* **1993**, *97*, 6477.
(16) Hayden, T. F.; Dumesic, J. A. *J. Catal.* **1987**, *103*, 366.
(17) Muijsers, J. C.; Weber, T.; Vanhardeveld, R. M.; Zandbergen, H. W.; Niemantsverdriet, J. W. *J. Catal.* **1995**, *157*, 698.
(18) Weber, Th.; Muijsers, J. C.; van Wolput, J. H. M. C.; Verhagen, C. P. J.; Niemantsverdriet, J. W. *J. Phys. Chem.* **1996**, *100*, 14144.
(19) Hermann, K.; Witko, M. In *Oxide Surfaces*; The Chemical Physics of Solid Surfaces; Woodruff, D. P., Ed.; Elsevier Science: Amsterdam, The Netherlands, 2001; Vol. 9, p 136.
(20) Kihlborg, L. *Acta Chem. Scand.* **1963**, *17*, 1485.
(21) Hermann, K.; Witko, M.; Michalak, A. *Catal. Today* **1999**, *50*, 567.
(22) Michalak, A.; Hermann, K.; Witko, M. *Surf. Sci.* **1996**, *366*, 323.
(23) Hammer, B.; Hansen, L. B.; Nørskov, J. K. *Phys. Rev. B* **1999**, *59*, 7413.
(24) Perdew, J. P.; Burke, K.; Ernzerhof, M. *Phys. Rev. Lett.* **1996**, *77*, 3865.
(25) Hermann, K.; Pettersson, L. G. M.; Casida, M. E.; Daul, C.; Goursot, A.; Koester, A.; Proynov, E.; St-Amant, A.; Salahub, D. R.; Carravetta, V.; Duarte, H.; Friedrich, C.; Godbout, N.; Guan, J.; Jamorski, C.; Leboeuf, M.; Leetmaa, M.; Nyberg, M.; Pedocchi, L.; Sim, F.; Triguero, L.; Vela, A. *StoBe Software*, 2009.
(26) Mars, P.; van Krevelen, D. W. *Chem. Eng. Sci.* **1954**, *3* (Spec. Suppl.), 41.
(27) Tokarz-Sobieraj, R.; Hermann, K.; Witko, M.; Blume, A.; Mestl, G.; Schlögl, R. *Surf. Sci.* **2001**, *489*, 107.
(28) Tokarz-Sobieraj, R.; Grybos, R.; Witko, M.; Hermann, K. *Collect. Czech. Chem. Commun.* **2004**, *69*, 121.
(29) Spevack, P. A.; McIntyre, N. S. *J. Phys. Chem.* **1993**, *97*, 11031.
(30) Delporte, P.; Meunier, F.; Pham-Huu, C.; Vennegues, P.; Ledoux, M. J.; Guille, J. *Catal. Today* **1995**, *23*, 251.

JP911639E